

Vertex reconstruction and tracking performance of the mSTS detector with the mCBM setup at SIS18

Dario Alberto Ramirez Zaldivar
(on behalf of the CBM Collaboration)^{a,b}

^a*GSI Helmholtzzentrum für Schwerionenforschung,
Planckstr 1, 64291 Darmstadt, Deutschland*

^b*Goethe University, Frankfurt, Deutschland*

E-mail: d.ramirez@gsi.de

The Compressed Baryonic Matter (CBM) experiment is one of the experimental pillars at the Facility for Antiproton and Ion Research (FAIR). The Silicon Tracking System (STS) is the central detector for track reconstruction and momentum measurement. It is designed to measure heavy ion collisions at interaction rates up to 10 MHz. It comprises approximately 900 double-sided silicon strip sensors with 1024 strips per side, arranged in 8 tracking stations in a magnetic field of 1 T · m bending power. In the context of the FAIR Phase-0 program, the mCBM setup at SIS18/GSI is a small-scale precursor of the full CBM experiment, consisting of pre-series productions of all major CBM detector subsystems aiming to verify CBM's concepts of free-streaming readout electronics, data transport, and online reconstruction. The mini-STs (mSTS) setup consists of 11 sensors arranged in 2 stations and no magnetic field.

Heavy ion collisions in the 1-2 AGeV/c range were measured with an average collision rate of 500 kHz. The primary and secondary vertices are reconstructed. Hit reconstruction efficiency was estimated using correlations with downstream detectors. This contribution will present the performance of hit, track, and vertex reconstruction from measurements of heavy-ion collisions.

*FAIR next generation scientists - 8th Edition Workshop (FAIRNESS 2024)
Sep 23–27, 2024
Donji Seget, Croatia*

1. Introduction

The Silicon Tracking System (STS) is the core detector for tracking and momentum determination of charged particles in the CBM experiment [1]. It is designed to reconstruct the trajectories for momentum determination with a resolution better than 2% and to reconstruct complex event topologies, such as the weak decays of strange or charmed hadrons and hypernuclei.

To reach event rates of up to 10 MHz, it uses fast and radiation-hard components, self-triggered front-end electronics, and a free-streaming readout architecture. A general detector description is given in [2, 3].

Prototype or pre-series components of all major CBM systems are installed in a common test setup, mini-CBM (mCBM), at the SIS18 synchrotron (GSI). The goals of mCBM focus on testing and optimizing the operation as a full system under realistic experimental conditions [4]. During beamtime campaigns in 2021 and 2022, heavy ion collisions (O+Ni, Ni+Ni, Au+Au) were measured at 2 AGeV/c, with an average collision rate of 500 kHz.

The mini-STs (mSTS) setup consists of 11 modules of two format sensor sizes: two with $62 \times 124 \text{ mm}^2$, 9 with $62 \times 62 \text{ mm}^2$. The system is laid out in 2 tracking stations of $12 \times 12 \text{ cm}^2$ and $18 \times 18 \text{ cm}^2$. A sketch top view of the mSTS and mCBM target chamber setup is shown in Fig. 1.

2. Data processing and testing

Prior to the installation in the mCBM cave, an energy calibration was performed to adjust the dynamic range of the ADC using a calibrated internal pulse generator and dedicated counters in the STS custom-designed front-end electronic [5]. The estimated baseline noise level corresponds to an Equivalent Noise Charge (ENC) below the targeted system noise of $1000 e$. Six modules were operated with relatively low thresholds, around $3 - 4\sigma$. The other five were operated with high threshold values due to the considerable noise. The typical particle rates were up to 28 kHz/channel.

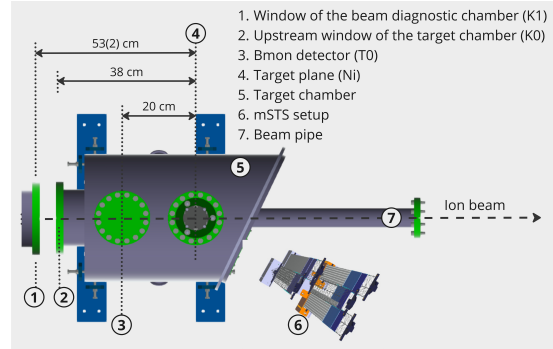


Figure 1: CAD top view of the target chamber of the mCBM setup highlighting the planes of interest for secondary interaction points.

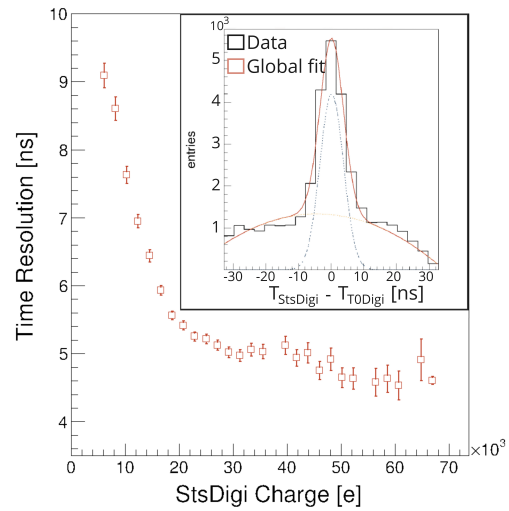


Figure 2: Estimated time resolution as a function of the STS signal amplitude. Fitted time difference distribution for large amplitude signal: ADC > 25.

The simplest decoded information from the recorded data files is the *StsDigi*: containing the address (module) and channel of the fired strip and time and charge information of the signal. Similar classes for all detection subsystems exist, adapted to the particularities of each detector. The STS *Clusters* are reconstructed by correlating signals from neighboring fired strips [6]. *Hits* are finally derived from the correlation of clusters on the p- and n-side [7] and fed to the tracking algorithm [8]. *Events* are defined using a seed detector and including all Digis within a time window, i.e., 60 ns for the STS. As a seed, a small diamond detector (T0) was used and placed in the beam upstream of the target. Typically, only one T0 hit is required to avoid event pile-up. A minimum of 8 TOF signals is demanded to remove empty or single-noise events, while events with more than 50 STS signals are removed to suppress massive noisy events from pick-up.

A time calibration is applied to raw signals before the cluster, hit, and event reconstruction. The time calibration corrects for potential offsets in the individual detector systems and for the time walk effect (the delay of the signal for lower signal amplitude). Removing this effect is crucial as the reconstruction algorithms are sensitive to it. The delay can span over 20 ns, distorting the output of the cluster finding algorithm [6]. The calibration ensures a proper synchronization within the detector resolution, which ranges between 4.6 and 9.2 ns, as shown in Fig. 2.

The space resolution is studied using the correlations of the hit position in the two tracking stations. The projection of the x-coordinate correlation peak is shown in Fig. 3. A mix of geometrical configuration, beam spot size, and detector resolution determines the width of the correlations. The agreement between Monte Carlo (MC) and data is remarkable, validating the simulations. By comparing these distributions, the detector resolution can be inferred to match the MC expectations. The estimated spatial resolution for a single strip cluster is $\sim 17 \mu\text{m}$, fulfilling the requirements for the CBM tracker.

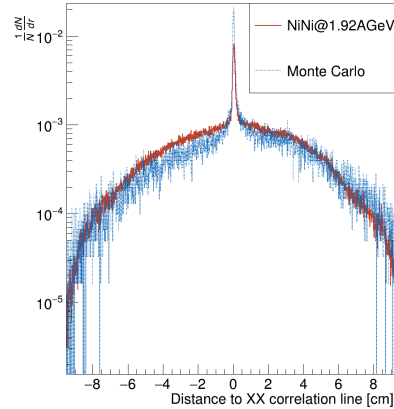


Figure 3: Distance to XX correlation line distribution compared to MC simulations.

3. Beam spot reconstruction

The setup has no magnetic field, so the track model is a straight line. The beam spot is reconstructed by track extrapolation to the target plane. Here, tracks are determined by two STS hits, one from each station. To reduce background and false combinations, events with low multiplicity are chosen (< 50 StsDigis). A selection of hits with amplitude larger than 20 ke is applied to suppress noise hits. This latter condition negatively impacts the tracking efficiency, but for the beam spot reconstruction, the purity of the signal was maximized. Figure 4(a) shows the XY distribution of two STS hit track extrapolation to the Ni target plane. The beam spot size, characterized by a Gaussian distribution with $\sigma_{irg}^X = 0.1583$ cm, $\sigma_{irg}^Y = 0.2167$ cm is compatible with the information extracted from the distribution measured by the T0 detector [4].

The beam spot reconstruction allows the identification of secondary interaction points of the beam with different elements of the Target Chamber, shown in Fig. 1. The X projections of the

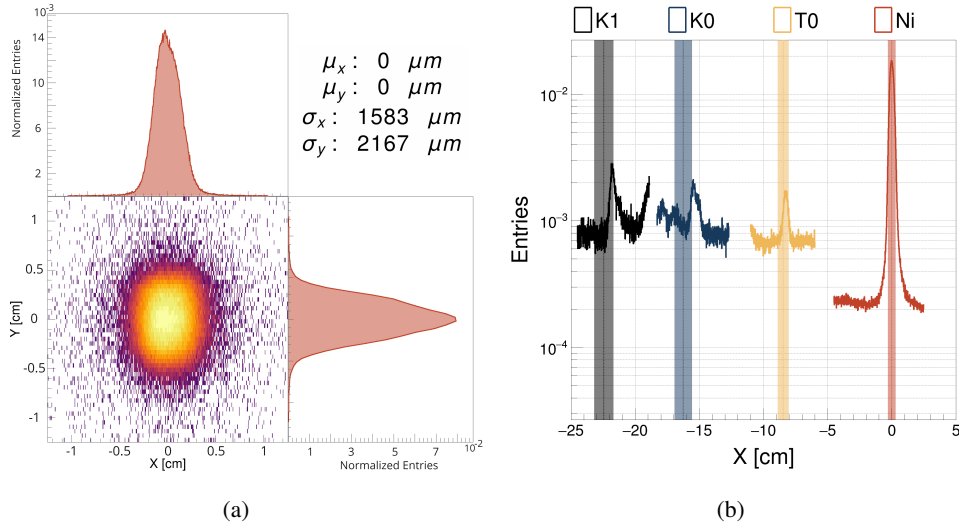


Figure 4: a) Beam spot reconstruction at the target plane by STS tracks. b) Projection along the x-axis for different z-planes, corresponding to secondary interaction points: window of the beam diagnostic chamber (K1), upstream window of the target chamber (K0), Bmon detector (T0), target (Ni).

track-lets extrapolations at different z-planes are shown in figure 4(b). The shadow boxes represent the nominal position of the distribution peaks, and their width reflects the propagated uncertainties. The systematic shift seen for K0 and K1 of the residual is compatible with a setup rotation of 1° around the y-axis.

4. Vertices reconstruction

Unlike the beam spot, which is determined as an average over multiple events, the event-by-event primary vertex estimates the primary interaction point for a single collision. The three-dimensional primary vertex is reconstructed using the Point of Closest Approach (PCA) method, which involves averaging the positions of all valid PCAs from track pairs in the event. A PCA is deemed valid if the distance between the point and the tracks is not significantly greater than the vertex resolution, typically on the order of hundreds of microns. The intention is to suppress false combinations between primary and secondary tracks. Track criterion of two STS hits, at least one TRD hit, and at least one TOF hit is required.

Figure 5(b) shows the PCA XZ projection distribution. Several structures can be appreciated. The interaction points of the beam with different elements upstream of the Ni target are visible and aligned along the beam axis. The interaction at this last one dominates the main contribution. Downstream, between 25 - 45 cm, structures arise from secondary particles produced by the mSTS setup material.

The result of such a simplistic approach is enough to locate different interaction points. Additionally, it provides a 3D event vertex reconstruction that requires no constraints on the target location, in contrast to the track extrapolation. The secondary tracks bias the precision of event vertex location, as DCA cuts cannot entirely suppress the contamination for primary event vertex estimation. This is appreciable by the difference between the beam spot shape and the XY projection of the estimated event vertex shown at figure 5(a).

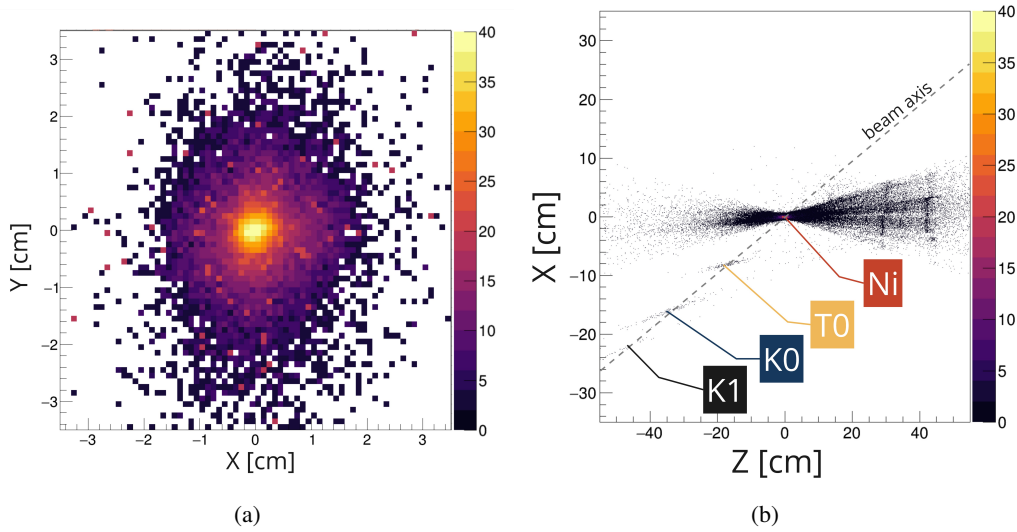


Figure 5: a) XY projection of the reconstructed 3D event vertex. b) XZ distribution for all valid PCA.

5. Summary

The mSTS detector, which employs two tracking stations to study heavy-ion collisions at SIS18, facilitates an evaluation that indicates the feasibility of attaining the targeted tracking performance level for the STS system. The system manifests commendable spatial and temporal resolution and proficient vertex capabilities.

References

- [1] K. Agarwal for the CBM Collaboration. The compressed baryonic matter experiment at fair—physics, status and prospects. *Physica Scripta*, 2023. doi: 10.1088/1402-4896/acbca7.
- [2] H. R. Schmidt. The silicon tracking system of the cbm experiment at fair. *Nuclear Instruments and Methods in Physics Research Section A: Accelerators, Spectrometers, Detectors and Associated Equipment*, 2019. doi: <https://doi.org/10.1016/j.nima.2018.09.094>. Frontier Detectors for Frontier Physics: 14th Pisa Meeting on Advanced Detectors.
- [3] A. Rodríguez Rodríguez. The silicon tracking system of cbm: towards tests with heavy ion collisions. *2019 IEEE Nuclear Science Symposium and Medical Imaging Conference (NSS/MIC)*, 2019. doi: 10.1109/nss/mic42101.2019.9059911.
- [4] C. Sturm, D. Emschermann, and N.Herrmann. Achievements of the mcbm beam campaign 2022, cbm progress report 2022. Technical report, 2022.
- [5] A. Rodríguez Rodríguez et. al. Functional characterization of modules for the silicon tracking system of the cbm experiment. *Nuclear Instruments and Methods in Physics Research Section A: Accelerators, Spectrometers, Detectors and Associated Equipment*, 2024. doi: <https://doi.org/10.1016/j.nima.2023.168813>.

- [6] V. Friese. A cluster-finding algorithm for free-streaming data. *EPJ Web of Conferences*, 2019. doi: 10.1051/epjconf/201921401008.
- [7] H. Malygina. *Hit reconstruction for the Silicon Tracking System of the CBM experiment*. PhD thesis, Universitätsbibliothek Johann Christian Senckenberg, 2018.
- [8] V. Akishina and I. Kisel. Online 4-dimensional reconstruction of time-slices in the cbm experiment. *IEEE Transactions on Nuclear Science*, 2015. doi: 10.1109/TNS.2015.2498099.